



A Report on
Experiments to Measure Average
Fibre Diameters by
Optical Fourier Analysis

J. R. Everett, D. M. O'Brien and T. J. Davis

DIVISION OF ATMOSPHERIC RESEARCH TECHNICAL PAPER No. 12
COMMONWEALTH SCIENTIFIC AND INDUSTRIAL
RESEARCH ORGANIZATION, AUSTRALIA 1986

A Report on
Experiments to Measure Average
Fibre Diameters by
Optical Fourier Analysis

By J. R. Everett, D. M. O'Brien and T. J. Davis

Division of Atmospheric Research Technical Paper No. 12

Commonwealth Scientific and Industrial
Research Organization, Australia

1986

A Report on Experiments to Measure Average Fibre Diameters
by Optical Fourier Analysis

J.R. Everett^{*}, D.M. O'Brien and T.J. Davis

CSIRO, Division of Atmospheric Research
Private Bag 1, Mordialloc, Victoria, 3195, Australia.

Abstract

This report outlines experiments to test whether the mean diameter of a sample of randomly oriented fibres can be inferred from observations of the power spectrum along a single ray in the Fourier plane. The report concludes that the obvious features of the power spectrum are uncorrelated with the mean diameter.

* Present address: Tasmanian Development Authority,
PO Box 6460, Hobart, Tas. 7001.

1. OVERVIEW

While studying the theory of diffraction, Thomas Young (1773 - 1829) proposed that the diameter of a hair fibre could be determined from its diffraction pattern. Indeed, there is an inverse relation between the diameter and the spacing of the minima of the diffraction pattern. In recent years Young's idea has been extended to a wide range of practical problems, ranging from determining the concentration of red blood cells to determining the size distribution of kerosene drops in fuel spray. In each of these applications the principle remains the same: objects in the sample contribute most strongly to the power spectrum at spatial frequencies inversely related to their size, and so by judiciously sampling the power spectrum one can infer the size distribution.

A typical experimental setup is shown in Figure 1. Light from a laser is expanded into a collimated beam, into the path of which is introduced the sample to be analysed. The image in the focal plane of the lens is the Fourier transform of the transmittance of the sample. Consequently, a detector which measures the intensity in the focal plane, but discards the phase, will record the power spectrum of the sample. Normally the focal plane will be partitioned into a number of regions, such as angular segments or annuli, and the power spectrum will be averaged over each of the regions. The partitioning is called a mask.

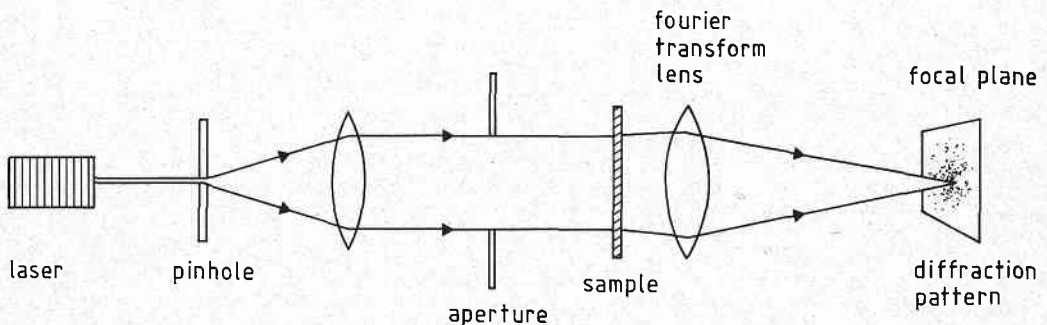


Figure 1: Typical experimental setup for an optical Fourier analyser.

As an example, suppose that the sample consists of circular particles with a range of sizes. The spectrum of each particle is axially symmetric and its amplitude is related to the Bessel function $J_1(2\pi rs)/s$, where s denotes the spatial frequency and r is the particle radius. The Bessel function has a central maximum at $s = 0$ and a sequence of decreasing maxima, whose spacing depends upon the size parameter r . Thus, by using an annular mask with radius at the spatial frequency of the first non-zero maximum, one might hope to detect particles with size r . The simplicity of this argument is deceptive, because the spectra generated by particles of different sizes interfere and may produce peaks at spatial frequencies which do not correspond to any of the particles present. Similarly, if the sample contains particles with a variety of shapes, then their spectra also interfere with equally confusing results.

In addition to these theoretical problems, there are certain practical problems, largely due to the wide dynamic range of the power spectrum. In particular:

- (1) the light intensity at high spatial frequencies may be many orders of magnitude less than the central peak;
- (2) the power spectrum is difficult to sample at low spatial frequencies;
- (3) the laser output usually fluctuates randomly.

Despite these well documented difficulties (Stark, editor (1982)), there are many applications where optical processing offers significant advantages because it is non-destructive and produces results in real time.

This report describes some experimental and theoretical work carried out at CSIRO division of atmospheric research (DAR) into the possibility of determining the mean diameter of wool fibres by optical Fourier analysis. The merits of such a scheme are obvious:

- (1) instantaneous processing, rather than laborious microscope analyses;
- (2) larger samples, leading to increased accuracy;
- (3) low cost instrumentation, which would be both rugged and easy to use, and consequently which could be installed in numerous field stations.

As an optical Fourier analyser had already been constructed at DAR for the purpose of analysing the size distribution of clouds from satellite imagery, it was decided to invest a small amount of research time into the proposal for determining wool sizes. Besides, wool is fluffy like clouds!

As already mentioned above, other attempts at determining size distributions from power spectra have used a mask in the two dimensional plane of the power spectrum. In the first series of experiments conducted at DAR and described in this report, we only sampled the power spectrum along a single line through the origin of the spectrum. Our reasons for this simplification were twofold:

- (1) it enabled us to use a single detector on a motorised stage rather than an expensive detector array;
- (2) if the fibre diameter could be correlated with some gross feature of the power spectrum, as we hoped it might, then it seemed reasonable that evidence of the correlation would survive in a one dimensional section of the power spectrum.

This hope proved to be unfounded, since both the theoretical and experimental work showed clearly that there is no simple correlation between the two.

Consider firstly the theoretical results. It is well known that a one dimensional scan of the spectrum is the one dimensional Fourier transform of the Radon transform of the object. The latter quantity is the function obtained by integrating the object along lines perpendicular to the direction of scan. We will give a simple example of fibres with a single diameter but whose Radon transform consists of blobs with a range of

diameters. We will also give a sequence of analytical results, starting with the power spectrum for a single straight fibre, and ending with the power spectrum of a collection of randomly oriented straight fibres with a range of diameters. For the first case, there is a clearly identifiable feature (the one observed by Young!) from which the fibre diameter can be inferred, but as the complexity of the sample is increased, the features which can be correlated with the fibre diameter are rapidly obscured.

Corresponding to each of these theoretical models, we constructed an experimental model from fine wires with known diameters and then verified the theoretical results in the laboratory. In addition, we processed wool samples obtained from the Australian Wool Testing Authority, but were unable to find any simple correlation between the one dimensional scan of the power spectrum and the fibre diameter.

Another avenue we explored was to reduce the two dimensional transform to a one dimensional transform by introducing a slit in front of the fibres. The attraction of this procedure was that the total length of the fibres in the slit could be related to the integral of the power spectrum, whereas the number of fibres could be related to its asymptotic rate of decay. Both of these quantities could be determined by integration of the power spectrum; a procedure which is generally stable. From the total length and the number of fibres, the average fibre diameter follows immediately. Although this procedure worked perfectly on numerical examples, the noise levels in the power spectrum prevented its practical application.

Our conclusion was that a useful measure of the fibre diameter could only be extracted from a one dimensional scan of the power spectrum when the fibres were fairly closely aligned and the range of diameters was small. Consequently, the device would probably be of more use in an industry such as the fibre glass industry where fibres are extruded, rather than the wool industry where sheep prefer wool with crimp.

Our analysis shows clearly why the simplistic treatment of the power spectrum is unsuccessful, and suggests that integration of the power spectrum around annuli would remove the dependence upon the orientation of the fibres. If so, the determination of the mean diameter of a random sample of wool fibres indeed might be possible. Further research (with increased experimental outlay) is needed to resolve this question.

Section 2 of this report outlines the theoretical analysis and experimental confirmation of the simple models. Section 3 contains details of the experimental setup. Section 4 presents the spectra obtained for the wool samples.

2 ANALYTICAL RESULTS

In this section we present a simple example to illustrate the implications of the 'projection - slice' theorem, which relates Fourier and Radon transforms. In addition, we consider some simple cases involving straight fibres which are amenable to exact analysis in order to form a basis for interpretation of the power spectrum.

We use the notation of Bracewell (1965) for Fourier transform pairs: functions of the spatial coordinates (x,y) are denoted by lower case Roman letters, such as $f(x,y)$, whereas the transformed function of the spatial frequency (u,v) is denoted by the corresponding upper case Roman letter, $F(u,v)$. We denote the power spectrum of $f(x,y)$ by $P(u,v)$.

2.1 Fourier and Radon transforms.

Consider a collection of fibres such as that illustrated in Figure 2a. Let $f(x,y)$ denote the function which is equal to one on the fibres and zero elsewhere. The Radon transform of f , denoted by \hat{f} , is defined by

$$\hat{f}(x) = \int dy f(x,y) .$$

Figure 2b shows the Radon transform of the fibres shown in 2a. Although the fibres have a common diameter, this dimension is obscured in the Radon transform, which consists of blobs with a variety of sizes. This observation is significant because the Radon transform is the one dimensional Fourier transform of the horizontal section through the spectrum of f . This is easy to see: the spectrum (Fourier transform) of f is

$$F(u,v) = \int dx \int dy \exp(-2\pi i(ux+vy)) f(x,y) .$$

Along the line $v = 0$, F reduces to

$$F(u,0) = \int dx \exp(-2\pi iux) \left(\int dy f(x,y) \right) ,$$

which is clearly equal to the one dimensional transform of \hat{f} . Because the Radon transform does not contain a single characteristic dimension, one might expect that a one dimensional scan through the power spectrum of f will not reveal a dominant spatial frequency. The results which follow will show that this is so.

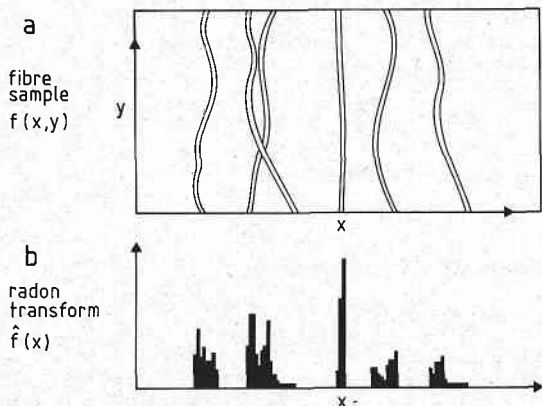


Figure 2: Radon transform of a sample of fibres.

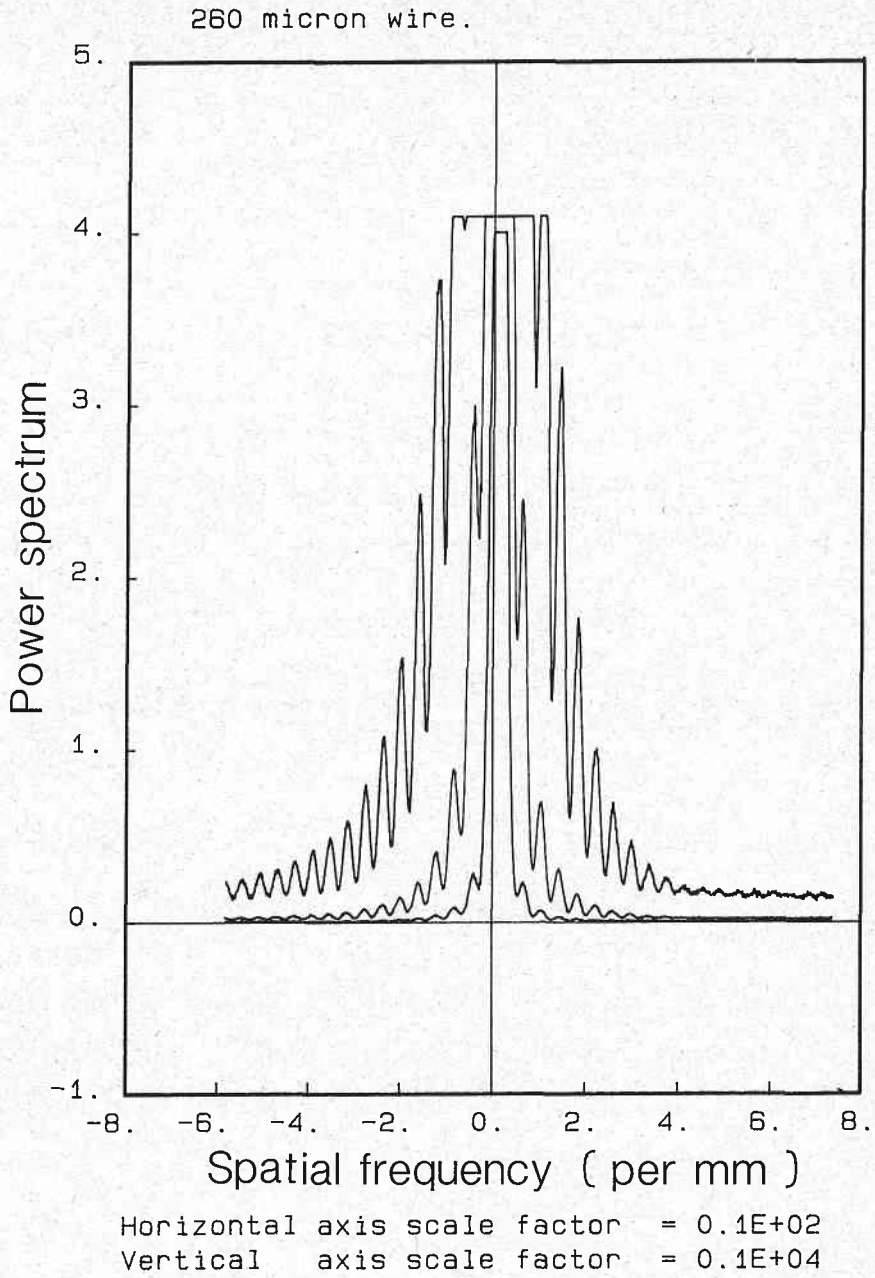


Figure 3: Power spectrum of a single fibre.

2.2 Single straight fibre.

Consider a fibre with centre (x_0, y_0) , diameter a and length b . Such a fibre may be represented by the boxcar function

$$f(x,y) = \Pi((x - x_0)/a) \Pi((y - y_0)/b) .$$

Its Fourier transform is

$$F(u,v) = \exp(-2\pi i u x_0) a \operatorname{sinc}(au) \exp(-2\pi i v y_0) b \operatorname{sinc}(bv) ,$$

and the corresponding power spectrum is

$$P(u,v) = a^2 \operatorname{sinc}^2(au) b^2 \operatorname{sinc}^2(bv) .$$

Along the line $v = 0$ where the power spectrum is sampled, the power spectrum reduces to

$$P(u,0) = a^2 b^2 \operatorname{sinc}^2(au) .$$

This function has zeros at a spacing of $1/a$, so the fibre diameter can be inferred from the spacing of the minima.

Figure 3 is an experimental observation of the power spectrum of a single wire. The three curves on the graph correspond to three different gain settings of the amplifier used to sample the spectrum. The minima are clearly visible. Measurement of their spacing leads to a diameter of 260 microns, in agreement with the value obtained with a micrometer.

2.3 Aligned fibres with a single diameter.

Suppose that the fibres have centres $(x_1, y_1), (x_2, y_2), \dots, (x_n, y_n)$. The object function, Fourier transform and power spectrum are now

$$f(x,y) = \sum_k \Pi((x-x_k)/a) \Pi((y-y_k)/b) ,$$

$$F(u,v) = a \operatorname{sinc}(au) b \operatorname{sinc}(bv) \sum_k \exp(-2\pi i (u x_k + v y_k)) ,$$

$$P(u,v) = a^2 \operatorname{sinc}^2(au) b^2 \operatorname{sinc}^2(bv) .$$

$$(n+2 \sum_{j>k} \cos 2\pi(u(x_j - x_k) + v(y_j - y_k))) .$$

The sinc functions now modulate a very rapidly oscillating function, whose frequencies are determined by the spacing between the fibres.

Figure 4 shows the experimental curve obtained with a sample of fine wires. Most of the rapid oscillation is averaged out by the limited spatial resolution of the detector, but some traces remain. The position of the minima of the sinc function are clearly visible, and the measurement of the spacing between the first minima yields a diameter of 50 microns. The diameter quoted by the manufacturer for the wires is 0.0016 inches, or 41 microns, although an attempt to measure the diameter with a micrometer gave 45 ± 5 microns. Since the wire was intended for winding fine coils, the quoted diameter is only a nominal figure and the diameter measured optically is almost certainly correct.

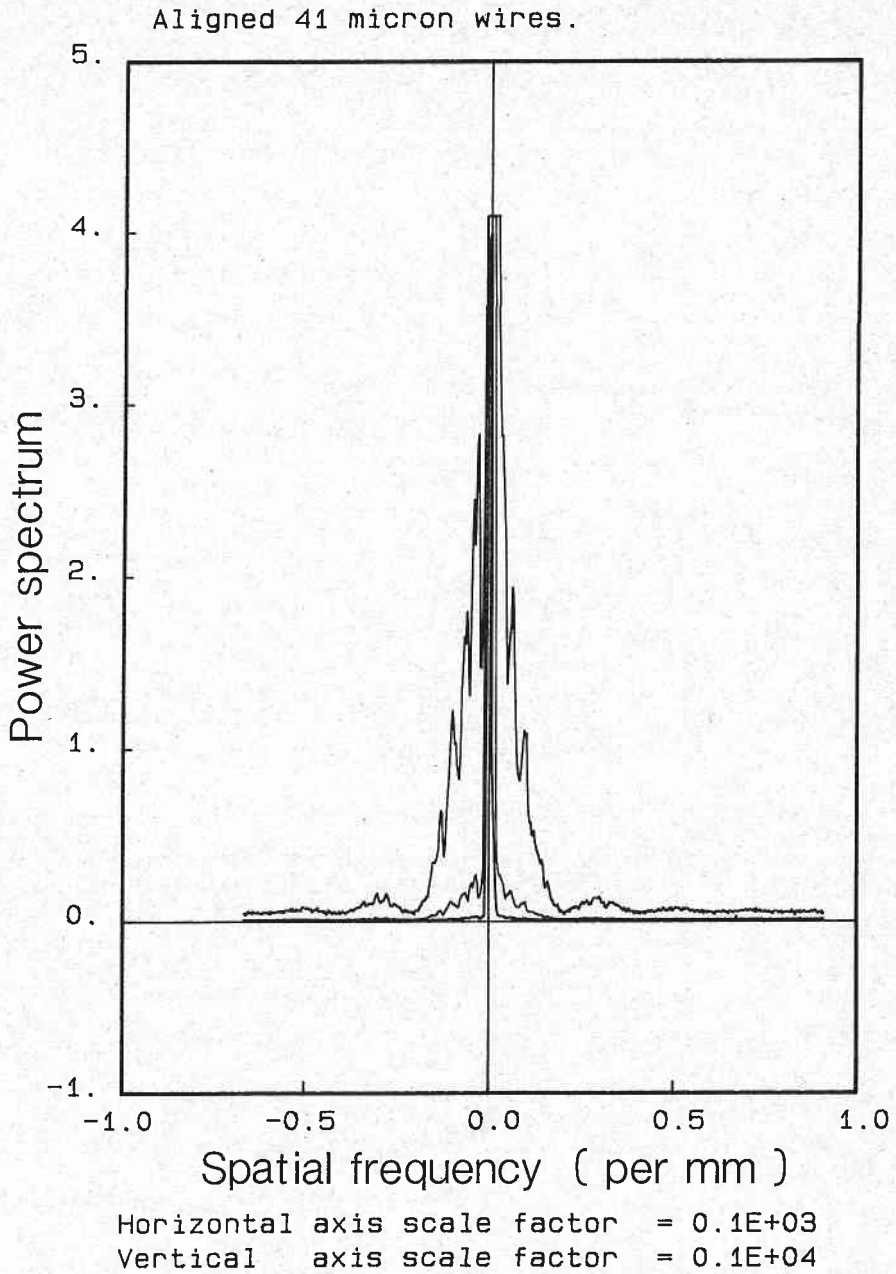


Figure 4: Power spectrum of aligned fibres with a single diameter.

2.4 Non-aligned fibres with a single diameter.

We now have

$$f(x,y) = \sum_k \Pi((+(x-x_k)\cos\theta_k + (y-y_k)\sin\theta_k)/a) \cdot \Pi((- (x-x_k)\sin\theta_k + (y-y_k)\cos\theta_k)/b),$$

where θ_k is the inclination of the k^{th} fibre to the vertical. Then

$$F(u,v) = \sum_k a \operatorname{sinc}(a(+u\cos\theta_k + v\sin\theta_k)) \exp(-2\pi i x_k (+u\cos\theta_k + v\sin\theta_k)) \cdot b \operatorname{sinc}(b(-u\sin\theta_k + v\cos\theta_k)) \exp(-2\pi i y_k (-u\sin\theta_k + v\cos\theta_k)),$$

$$P(u,v) = a^2 b^2 \left(\sum_k \operatorname{sinc}^2(a(+u\cos\theta_k + v\sin\theta_k)) \operatorname{sinc}^2(b(-u\sin\theta_k + v\cos\theta_k)) \right. \\ \left. + 2 \sum_{j>k} \operatorname{sinc}(a(+u\cos\theta_j + v\sin\theta_j)) \operatorname{sinc}(b(-u\sin\theta_j + v\cos\theta_j)) \cdot \operatorname{sinc}(a(+u\cos\theta_k + v\sin\theta_k)) \operatorname{sinc}(b(-u\sin\theta_k + v\cos\theta_k)) \cdot \right. \\ \left. \cos 2\pi((+u\cos\theta_j + v\sin\theta_j)x_j - (-u\sin\theta_j + v\cos\theta_j)y_j - (+u\cos\theta_k + v\sin\theta_k)x_k + (-u\sin\theta_k + v\cos\theta_k)y_k) \right).$$

Because the length to diameter ratio of the fibres is large, the sinc function involving the length is very small unless its argument is close to zero. Consequently, the cross terms in the power spectrum will be small in comparison with the diagonal terms, so, to an excellent approximation,

$$P(u,v) = a^2 b^2 \sum_k \operatorname{sinc}^2(a(+u\cos\theta_k + v\sin\theta_k)) \operatorname{sinc}^2(b(-u\sin\theta_k + v\cos\theta_k)), \\ = a^2 b^2 \sum_k \operatorname{sinc}^2(as \cos(\zeta - \theta_k)) \operatorname{sinc}^2(bs \sin(\zeta - \theta_k)).$$

Here we have introduced polar coordinates (s, ζ) in the Fourier plane:

$$u = s \cos \zeta,$$

$$v = s \sin \zeta.$$

Figure 5 shows that a minimum can still be detected, but its position is not so clearly defined. The diameter inferred from the spacing of the minima for this sample is 48 microns, in reasonable agreement with the value of 50 microns obtained above.

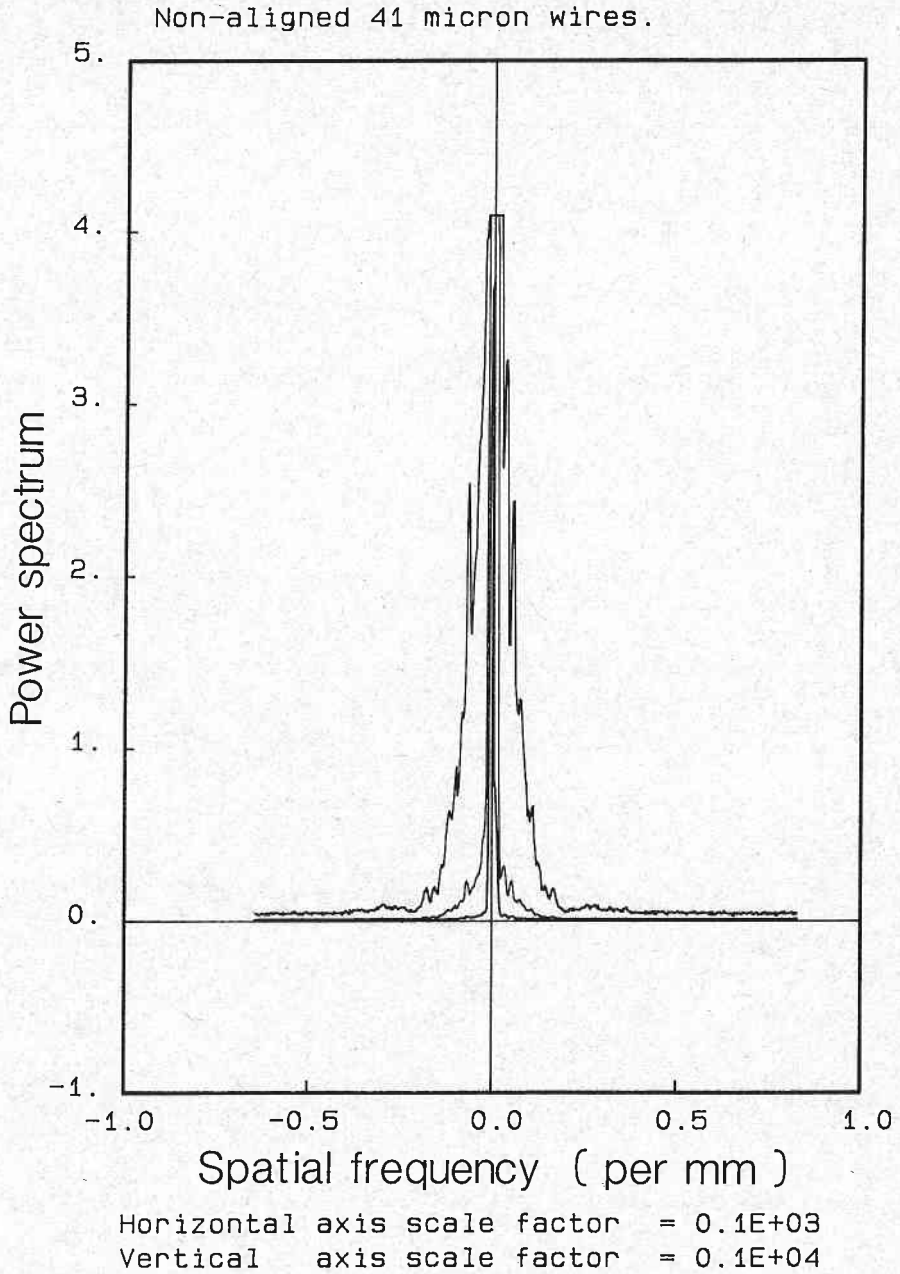


Figure 5: Power spectrum of non-aligned fibres with a single diameter.

2.5 Aligned fibres with a range of diameters.

Suppose now that the fibres have centres $(x_1, y_1), (x_2, y_2), \dots, (x_n, y_n)$, diameters a_1, a_2, \dots, a_n , and lengths b_1, b_2, \dots, b_n . Then

$$\begin{aligned}
 f(x, y) &= \sum_k \Pi((x-x_k)/a_k) \Pi((y-y_k)/b_k), \\
 F(u, v) &= \sum_k a_k \operatorname{sinc}(a_k u) \exp(-2\pi i u x_k) \cdot \\
 &\quad b_k \operatorname{sinc}(b_k v) \exp(-2\pi i v y_k), \\
 P(u, v) &= \sum_k a_k^2 b_k^2 \operatorname{sinc}^2(a_k u) \operatorname{sinc}^2(b_k v) \\
 &\quad + 2 \sum_{j>k} a_j a_k \operatorname{sinc}(a_j u) \operatorname{sinc}(a_k u) \cdot \\
 &\quad \quad b_j b_k \operatorname{sinc}(b_j v) \operatorname{sinc}(b_k v) \cdot \\
 &\quad \quad \cos 2\pi(u(x_j - x_k) + v(y_j - y_k)).
 \end{aligned}$$

If the interference between the spectra of separate fibres is neglected, then

$$P(u, v) = \sum_k a_k^2 b_k^2 \operatorname{sinc}^2(a_k u) \operatorname{sinc}^2(b_k v),$$

and along the line $v = 0$

$$P(u, 0) = \sum_k a_k^2 b_k^2 \operatorname{sinc}^2(a_k u).$$

The power spectrum no longer has zeros which can be related to the fibre diameter.

In order to carry the analysis further, suppose that the diameters are drawn from a beta distribution, so that the number of fibres with diameters in the range from a to $a+da$ is

$$n(a) da = (a/c)^{p-1} (1-a/c)^{q-1} / B(p, q) d(a/c).$$

Here p and q are parameters defining the distribution, c is the maximum fibre diameter in the sample, and $B(p, q)$ is the beta function. Then,

$$P(u, 0) = \int da n(a) a^2 b^2 \operatorname{sinc}^2(au),$$

where we have assumed that the fibres have the same length. This integral reduces to

$$P(u, 0) = 2(b/(2\pi u))^2 (1 - \operatorname{Re} \phi(p, p+q, -2\pi i c u)),$$

where ϕ is the confluent hypergeometric function. For large u ,

$$P(u, 0) = 2(b/(2\pi u))^2 (1 - \cos(\pi p/2) / (\Gamma(q) (2\pi c u)^p)).$$

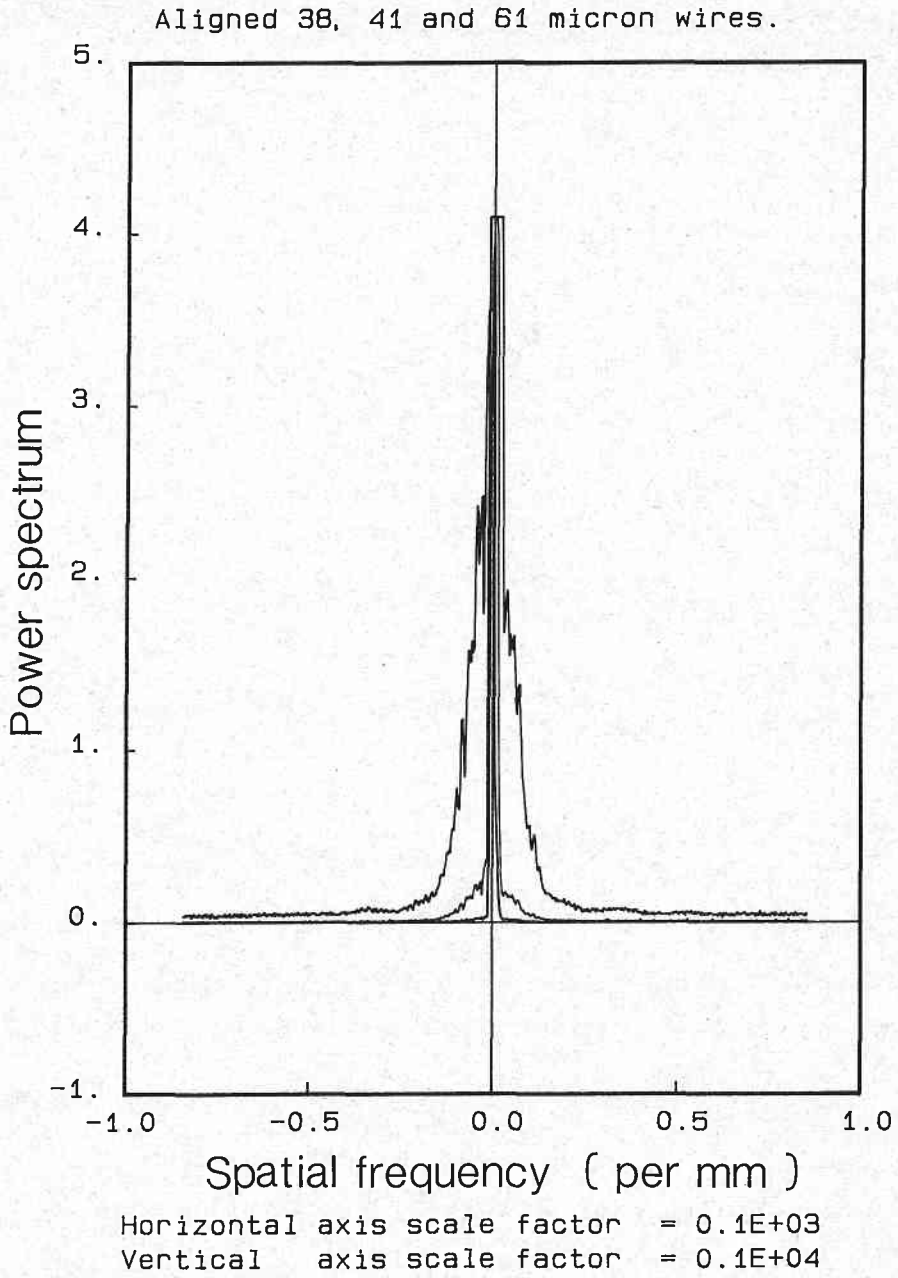


Figure 6: Power spectrum of aligned fibres with several diameters.

From the value of the power spectrum at the origin, the analytical form involving ϕ , and the asymptotic behaviour for large u , four parameters must be determined, namely b , c , p , q . In terms of the parameters, the mean fibre diameter is

$$\langle a \rangle = \int n(a) a da = c p / (p+q).$$

In principle a least squares fitting procedure ought to recover the parameter values. This technique was considered by O'Brien (1986) in another context, but the results of numerical simulations were not encouraging due to the rapid oscillation of the power spectrum.

Figure 6 shows the experimental results for a sample consisting of parallel wires with three diameters, 38, 41, and 61 microns, mixed in approximately equal numbers. As expected, the power spectrum does not have zeros which can be related simply to an average fibre diameter.

2.6 Non-aligned fibres with a variety of diameters.

In this most general case,

$$f(x,y) = \sum_k \Pi((+(x-x_k) \cos \theta_k + (y-y_k) \sin \theta_k) / a_k) \cdot \\ \Pi((- (x-x_k) \sin \theta_k + (y-y_k) \cos \theta_k) / b_k), \\ F(u,v) = \sum_k a_k \operatorname{sinc}(a_k (+u \cos \theta_k + v \sin \theta_k)) \cdot \\ \exp(-2\pi i x_k (+u \cos \theta_k + v \sin \theta_k)) \cdot \\ b_k \operatorname{sinc}(b_k (-u \sin \theta_k + v \cos \theta_k)) \cdot \\ \exp(-2\pi i y_k (-u \sin \theta_k + v \cos \theta_k)), \\ P(u,v) = \sum_k a_k^2 \operatorname{sinc}^2(a_k (+u \cos \theta_k + v \sin \theta_k)) \cdot \\ b_k^2 \operatorname{sinc}^2(b_k (-u \sin \theta_k + v \cos \theta_k)) \\ + 2 \sum_{j>k} a_j \operatorname{sinc}(a_j (+u \cos \theta_j + v \sin \theta_j)) \cdot \\ b_j \operatorname{sinc}(b_j (-u \sin \theta_j + v \cos \theta_j)) \cdot \\ a_k \operatorname{sinc}(a_k (+u \cos \theta_k + v \sin \theta_k)) \cdot \\ b_k \operatorname{sinc}(b_k (-u \sin \theta_k + v \cos \theta_k)) \cdot \\ \cos 2\pi((+u \cos \theta_j + v \sin \theta_j) x_j - (-u \sin \theta_j + v \cos \theta_j) y_j \\ - (+u \cos \theta_k + v \sin \theta_k) x_k + (-u \sin \theta_k + v \cos \theta_k) y_k)).$$

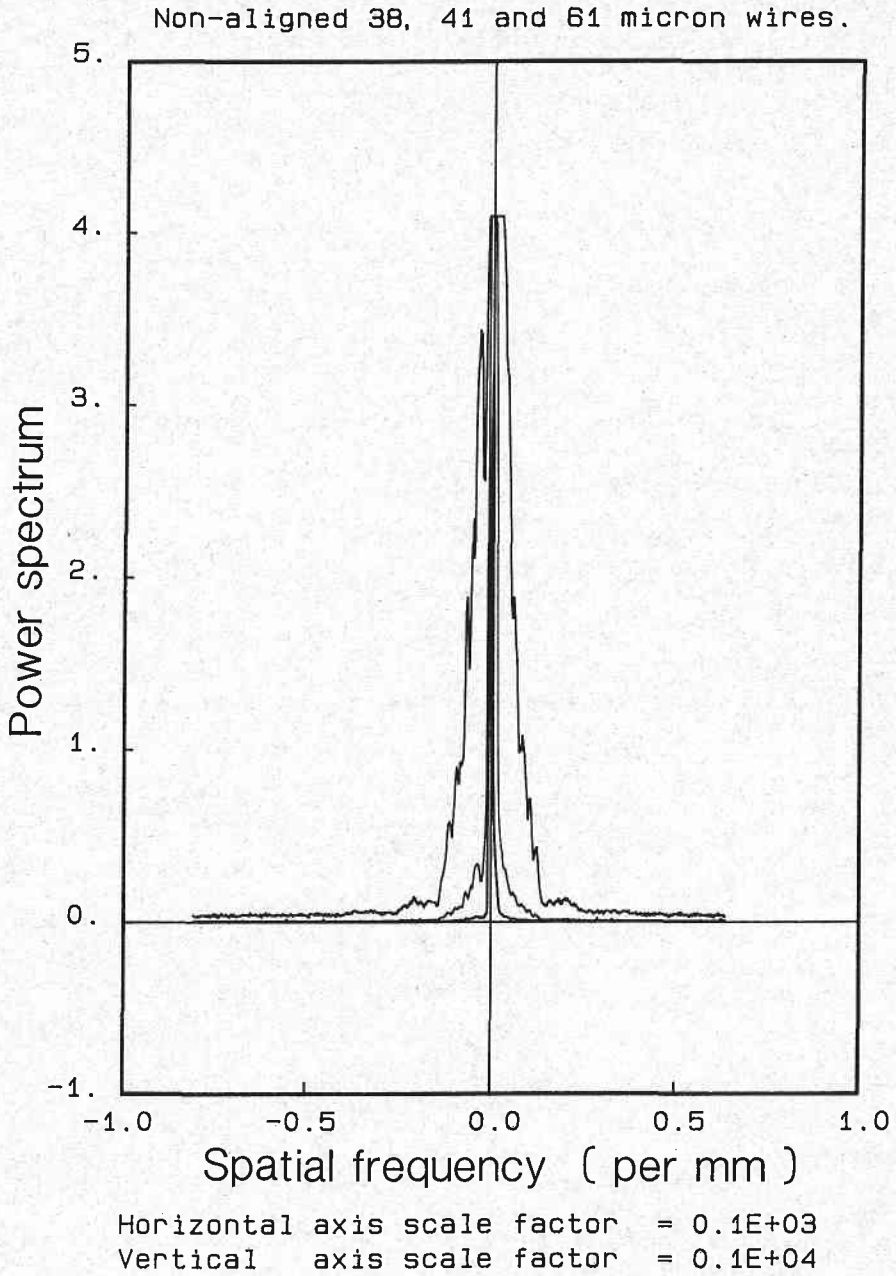


Figure 7: Power spectrum of non-aligned fibres with several diameters.

Again the interference between fibres may be neglected and so

$$P(u,v) = \sum_k a_k^2 \operatorname{sinc}^2(a_k(+u\cos\theta_k + v\sin\theta_k)) \\ b_k^2 \operatorname{sinc}^2(b_k(-u\sin\theta_k + v\cos\theta_k)) \quad ,$$

and along the line $v = 0$

$$P(u,0) = \sum_k a_k^2 \operatorname{sinc}^2(a_k u \cos\theta_k) b_k^2 \operatorname{sinc}^2(b_k u \sin\theta_k) \quad .$$

Figure 7 is the experimental power spectrum obtained with a sample consisting of approximately equal numbers of wires with diameters of 38, 41 and 61 microns. All evidence of a minimum has faded from the plot.

2.7 One dimensional analysis.

If a horizontal slit is placed in front of vertically running fibres, then the spectrum is the one dimensional Fourier transform of the fibres in the slit window. Let $f(x)$ denote the function equal to one on the fibres in the slit window and zero elsewhere. The total length of fibre in the slit window is

$$L = \int f(x) dx \quad ,$$

and this quantity is related to the integral of the power spectrum. Indeed,

$$L = \int P(u) du \quad .$$

Also, it is possible to prove (O'Brien (1986)) that the number N of fibres in the slit window is given by

$$N = \lim_{X \rightarrow \infty} \pi^2/X \int_{-X}^X u^2 P(u) du \quad .$$

Since the mean fibre diameter is

$$\langle a \rangle = L/N \quad ,$$

it can, in principle, be determined by integration of the power spectrum, a process which is usually numerically stable. If successful, this method would allow accurate determination of the average diameter of aligned fibres, no matter how wide the range of diameters in the sample. This procedure worked well in numerical simulations, but failed in practice because the signal to noise ratio was too small at the high spatial frequencies needed to compute the number of fibres in the sample.

3. EXPERIMENTAL SETUP

The apparatus is essentially the same as that given in figure 1. A parallel beam of light from a He - Ne laser falls on the sample whose fibres are aligned as closely as possible with the vertical. In front of the sample is an optional horizontal slit of about 0.5mm width. The lens creates a Fraunhofer diffraction pattern of the sample and the slit in the focal plane of the lens. The detector consists of a pin hole, with diameter approximately equal to 100 microns, and a photo-transistor which has a built in lens over the silicon chip. Consequently, all the light energy which passes through the pinhole is collected by the photo-transistor. Three cascaded operational amplifiers produce three outputs with a gain of about 11 between each stage. The pin hole, photo-transistor and amplifiers are mounted on a motorised stage which is used to scan the detector at a constant rate across the diffraction pattern. The stage motor produces a pulse for every 0.1 microns travelled, so the position of the detector is determined by counting the pulses, and consequently is known with high precision.

The amplifier circuit is shown in Figure 8. The variable resistors are used to adjust DC offsets in the circuit, and the zener diodes are used to limit the input voltage into the analogue of digital converter. The 1.9M and 1 μ F feedback impedance of the first amplifier could be switched out and a series of other resistor/capacitor combinations, and hence other gains, could be substituted. However, for the experiments described herein only the values shown were used.

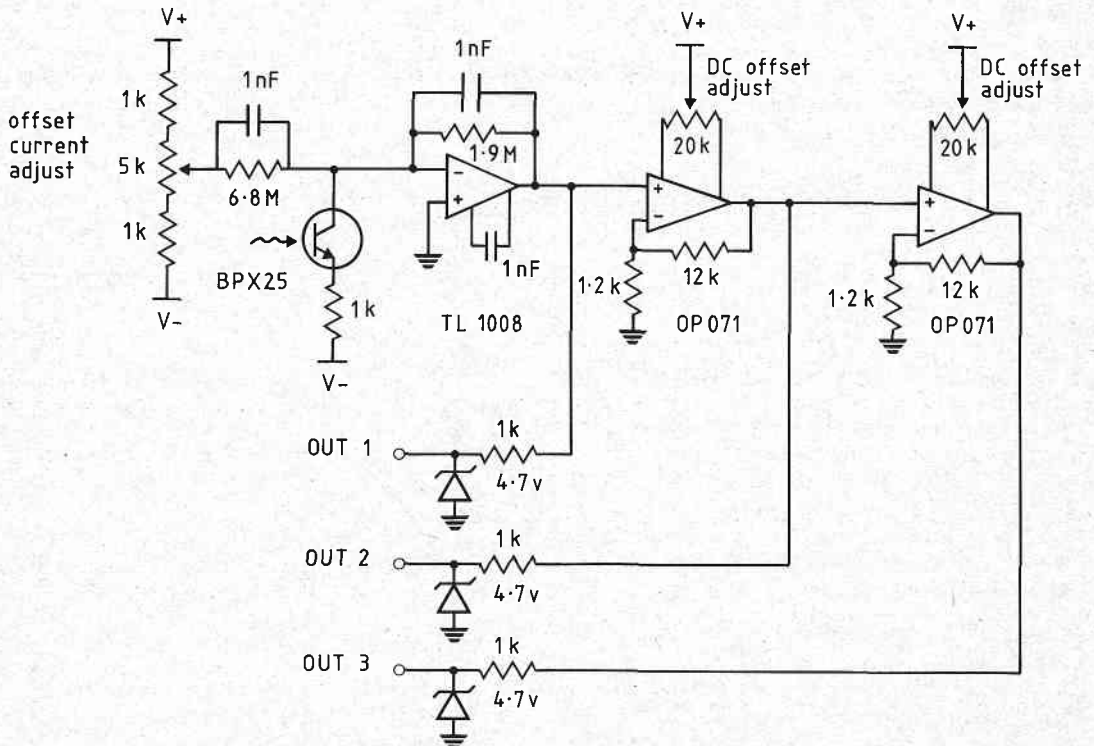


Figure 8: Amplifier circuit.

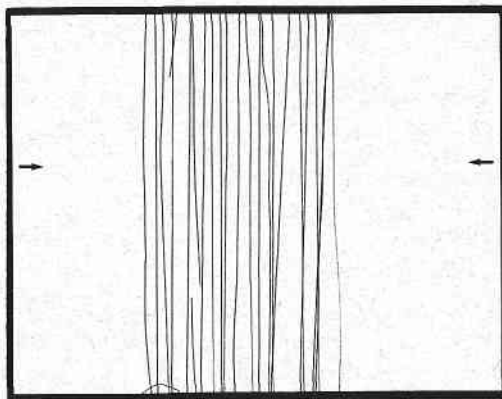
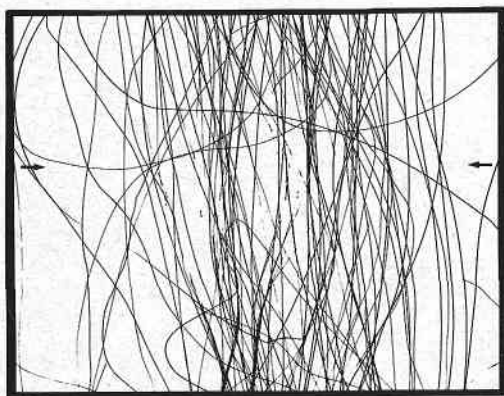
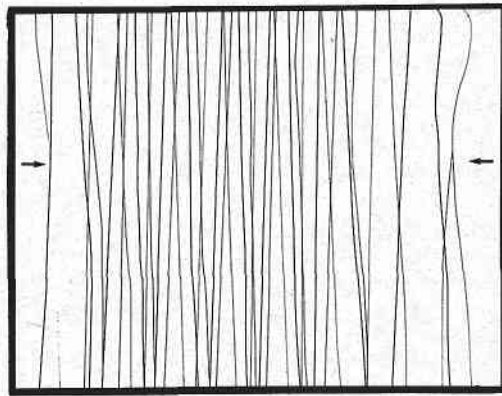
41 μm 41 μm 38, 41 & 61 μm 38, 41 & 61 μm

Figure 9: Wire samples.

Before each experiment, the offsets in the amplifiers were adjusted to be slightly above zero, so that the output signals would remain positive even if the amplifiers drifted. This was necessary because the A/D converter only digitises positive voltages. The photo-transistor aperture was covered at the beginning and at the end of each scan in order to find values for the DC offsets.

The detector was centred on the central spot of the diffraction pattern and the optical slit was aligned as closely as possible with the scan line of the motorised stage. Alignment errors cause asymmetries in the measured diffraction patterns, which should be even functions of spatial frequency. The detector was moved well away from the central spot and then data was collected as the detector moved across the diffraction pattern, through the central region, and out to the opposite extreme. Data was taken after every 128 or 256 pulses from the stage motor, or every 12.8 or 25.6 microns. The three outputs from the circuit were digitised by a 12 bit A/D converter and stored on floppy disk. Each scan took about five minutes to complete.

The three channels of data were subsequently plotted as functions of the spatial frequency, which is related to the label k of the sample by

$$u = k p / (\lambda f) ,$$

where f is the focal length of the lens, λ is the wavelength of the light, and p is the number of motor pulses between data samples. The zero point for spatial frequency was chosen to coincide with the central maximum of the diffraction pattern.

Figure 9 shows the wire samples used for the test runs. Sample #1 consisted of 41 micron diameter wire wound around a photographic slide holder so that the wires were approximately evenly spaced and were approximately vertical. Sample #2 was the same wire, but scatter wound onto the slide and kinked. The aim was to produce a sample of wires with a single diameter that represented a wool sample. Sample #3 was similar to sample #1, except that three different wire sizes were wound together, thus giving a distribution of diameters. The wire diameters were 38 microns, 41 microns and 61 microns. Sample #4 was wound in a similar way to sample #2, but the three wire sizes were used. In all samples, between 20 and 40 wires were illuminated and formed the diffraction pattern.

4. WOOL SAMPLES

Eight samples of classed wool from the Australian Wool Testing Authority were analysed, both with and without the horizontal slit mentioned above. The nominal mean diameters for the samples were 18.5, 20.2, 22.3, 23.6, 26.3, 28.4, 29.5, 33.4 microns. Figures 10 and 11 show for 18.5 micron wool the raw data set and a normalised data set, obtained by selecting the most sensitive, non-saturated output from the three amplifiers. These curves are typical for all the wool sizes tested. None of the curves shows any pronounced feature, such as a minimum, which might be correlated with the fibre diameter. The widths of the normalised curves, measured at half height, and the nominal fibre diameters are listed in the Table below.

Table: A comparison of fibre diameter with measured peak widths.

Fibre diameter (microns)	Width of peak at half height (arbitrary units)	
	Slit	No slit
18.5	0.75	0.75
20.2	0.65	0.70
22.3	0.65	0.75
23.6	0.70	0.75
26.3	0.60	0.70
28.4	0.80	0.75
29.5	0.65	0.70
33.4	0.85	0.60

The correlation between width of the peak in the power spectrum and the fibre diameter is 0.42 for the experiment with the slit and -0.67 in the experiment without the slit. It is clear that this technique is useless for measuring the average diameter of wool fibres.

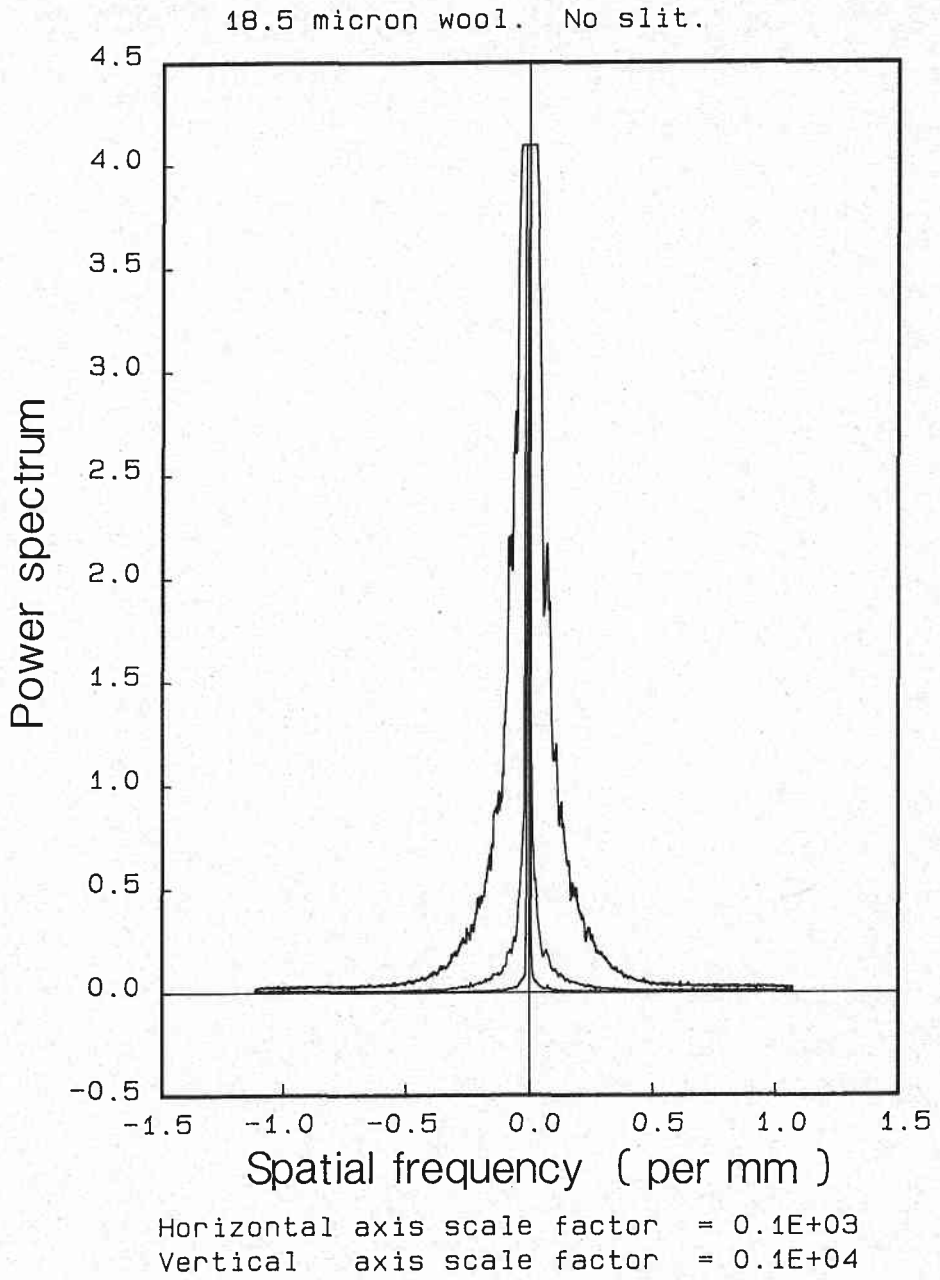


Figure 10: Power spectrum for 18.5 micron wool: unprocessed.

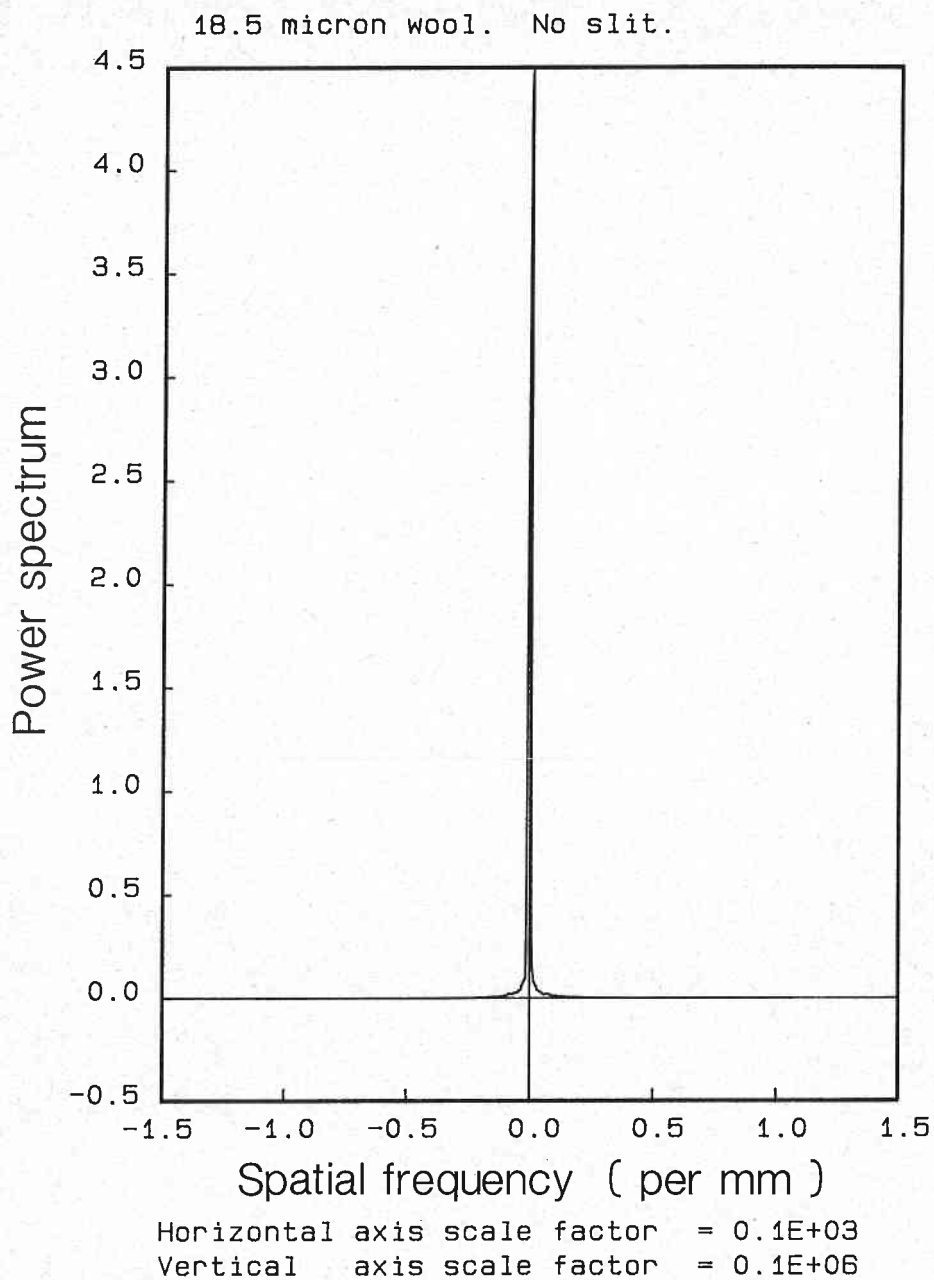


Figure 11: Power spectrum for 18.5 micron wool: processed.